



17th CIRP Conference on Modelling of Machining Operations

Numerical Modelling of Cutting Forces in Gear Skiving

Bruno Vargas*, Matthias Zapf, Jan Klose, Frederik Zanger, Volker Schulze

*wbk Institute of Production Science, Karlsruhe Institute of Technology (KIT), Kaiserstr. 12, 76131 Karlsruhe, Germany** Corresponding author. Tel.: +49 721 608-42447; fax: +49 721 608-45004. E-mail address: bruno.vargas@kit.edu**Abstract**

Gear skiving is a high-performance machining process for gear manufacturing. Due to its complex kinematics, the local cutting conditions vary during tool engagement. Particularly, the local rake angle can reach highly negative values, which have a significant effect on the cutting force. In this paper, the Kienzle force model with additional coefficients was implemented in a numerical model to calculate local cutting forces considering the influence of local rake angle. The experimental validation based on total cutting forces shows good results and indicates an increase of model accuracy for a wide parameter range by considering the rake angle variation.

© 2019 The Authors. Published by Elsevier B.V.

Peer-review under responsibility of the scientific committee of The 17th CIRP Conference on Modelling of Machining Operations

Keywords: Machining, Gear manufacturing, Kinematic force modelling**1. Introduction**

Gear skiving is a highly productive machining process for the manufacture of internal and external gears. In comparison to other established processes for internal gears, like gear shaping and broaching, it offers advantages in flexibility and productivity. Moreover, it is also largely used in the manufacture of components with internal and external gearings.

Gear skiving is especially attractive for the production of gears with interfering contours, since the tool overrun can be diminished by reducing the axis crossing angle. In this particular case, higher spindle rotations are needed to compensate the diminution of the cutting speed. Furthermore, the local rake angle can reach large negative values due to the unfavorable kinematics, which has a negative impact on the cutting forces.

The gear skiving was patented in 1910 [1] but its industrial establishment was only possible many years later with the introduction of new technologies in the machine tool industry and especially with the development of simulative approaches to the process design. Jansen [2] first investigated the gear skiving kinematics and Hühsam [3] proposed a mathematical model for tool and process design, providing an extensive investigation of the influence of tool geometry and process parameters on the local cutting conditions. The influence of the different process parameters was investigated in other recent works [4, 5, 6, 7, 8].

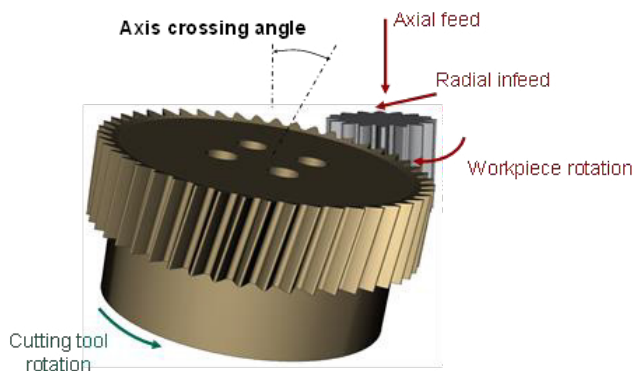


Fig. 1. Main process parameters of gear skiving.

Nomenclature	
A_c	Cross-sectional area of cut
b	Width of cut
C_M	Model fitting coefficient for cutting speed, chip deformation and tool wear
d_a	External diameter
F_c	Cutting force
h	Uncut chip thickness
h_{max}	Maximum uncut chip thickness
m_c	Exponent of cutting force
i	Index for position along the cutting trajectory
j	Index for points along the cutting edge
k_c	Specific cutting force
k_{c11}	Nominal specific cutting force
k_{chip}	Chip deformation coefficient
k_{vc}	Cutting speed coefficient
k_{wear}	Tool wear coefficient
k_γ	Rake angle coefficient
m_b	Normal module
r_b	Base diameter of workpiece
S_{ax}	Axial feed
$S_{ax,t}$	Axial translation between consecutive cuts
v_c	Cutting speed
v_s	Sliding speed
z_0	Number of teeth of cutting tool
z_2	Number of teeth of workpiece
α	Clearance angle
α_{tool}	Tool clearance angle
β_b	Base helix angle
β_0	Helix angle of cutting tool
β_2	Helix angle of workpiece
$\Delta\varphi$	Angular increment between consecutive cuts
γ	Rake angle
γ_{min}	Minimum rake angle
γ_{tool}	Tool rake angle
γ_{local}	Local rake angle
K	Tilt angle
Σ	Axis crossing angle

The skiving process is characterized by variable local cutting conditions: cutting and sliding speeds, uncut chip thickness, clearance and rake angles result from the complex gear skiving kinematics and the process parameters vary along the cutting edge and during the tool engagement as well. These do not vary linearly with the process parameters and represent a great challenge for the process design. In order to enhance the efficiency of the skiving process design, the understanding of cutting forces is needed.

The calculation of process forces provides a valuable tool for improving the process and machine tool design, shortening development times and setting a high level of process reliability. However, there is still a lack of knowledge about the influence of the local cutting conditions, especially the local rake angle, on the cutting forces.

1.1. Modeling of cutting forces

Jansen [2] first investigated the skiving process in terms of kinematics, proposing the first simulative approach for the cutting force calculation based on empirical results for turning. Also based on fundamentals of metal cutting, Spath and Hühsam [9] proposed a model for calculating the cutting forces by gear skiving using the Kienzle equation. The forces are calculated from the specific cutting force and cross-sectional area for discrete elements along the cutting edge and then summed up without considering the influence of local cutting conditions other than the uncut chip thickness. For instance, the influence of the local rake angle is not considered in this model. A more recent work of Kühlewein [4] used a FEM-based analysis of the skiving process focusing on the chip formation mechanism to calculate temperature and the cutting forces.

Li et al. [10] proposed a method for calculating the cutting forces by gear skiving using the energy method. Guo et al. [8] developed a cutting model based on material mechanics and investigated the influence of multiple-infeed strategies on the skiving performance. Nevertheless, these models consider many material properties, which cannot be easily determined. This impairs their practical application in process design.

1.2. Influence of the rake angle on the cutting forces

In gear skiving, the rake angle can reach large negative values due to its kinematics. Differently from profile milling and gear hobbing, the workpiece rotation reaches high values and the correspondent kinematics result, inter alia, in large negative rake angles. Especially in skiving of external gears and with reduced axis crossing angles, the local rake angles become critical because of the unfavorable kinematics [3].

The friction coefficient on the rake face can double in orthogonal cutting with negative rake angles smaller than $\gamma < -55^\circ$ [11]. Because of the increase of the tool-chip friction factor τ/k , the ratio between deformed chip and uncut chip thicknesses also increases [12]. The larger contact area and the high chip volume lead to increased cutting forces [13].

The cutting forces can be calculated from the specific cutting force k_c and cross-sectional area of cut A_c . However, the specific cutting force k_c depends not only on the workpiece material, but also varies logarithmically with the uncut chip thickness. Originally, the Kienzle equation correlates the nominal specific cutting force $k_{c1,1}$ and the correspondent exponent m_c , which are material properties and can be found in the literature or are experimentally determined, with the uncut chip thickness h . Additionally, the influences of the cutting speed, chip formation, material removal rate, tool wear and rake angle can be also considered. Thus, the extended Kienzle equation is given by:

$$k_c = (k_{vc} \cdot k_{chip} \cdot k_{wear} \cdot k_\gamma) \cdot k_{c1,1} \cdot h^{-m_c} \quad (1)$$

Different approaches to quantify the influence of the rake angle on the cutting force can be found in literature [13, 14, 15, 16]. The approach described by Apprigh et al. [14] and Dietrich [15] considers a linear variation of the cutting forces with the rake angle, in which the cutting forces vary 1 % per degree rake

angle change. The second approach, described by Saglam et al. [13] and Günay [16] considers that the cutting forces vary 1.5 % per degree rake angle change. These relations are mathematically expressed by the following equations:

$$k_{\gamma,AD} = 1 - \frac{\gamma-6}{100} \quad (2)$$

$$k_{\gamma,GS} = 1 - \frac{109-1.5\cdot\gamma}{100} \quad (3)$$

2. Numerical procedure

The local cutting conditions uncut chip thickness, cutting and sliding speed, clearance and rake angle result from the gear skiving kinematics and the process parameters. Those vary along the cutting edge and during the tool engagement as well.

In order to calculate the local cutting conditions, an iterative model of the skiving process based on Hühsam [3] was implemented. The cutting tool tooth profile is modelled as a point cloud and its movement relative to a fixed workpiece is calculated. Furthermore, the tool angles (helix angle, tool rake and clearance angles) and the data from cutting tool/workpiece arrangement (axis crossing angle, center distance and tilt angle) are also represented in the calculation of the cutting trajectory and the correspondent local cutting conditions.

The gearing mechanism is represented through only one moving body for each cutting tool pass, simplifying the calculation by reducing the number of variables. Then the cutting trajectories for two consecutive tooth engagements in one gap between teeth are compared to determine the penetration volume (figure 2a). For the same radial infeed and constant axial feed, each cut performed by the tooth of the cutting tool is identical. For that reason, the second cutting trajectory corresponds to a combination of axial translation $S_{ax,t}$ and rotation $\Delta\varphi_0$ of the first one.

$$S_{ax,t} = S_{ax} \frac{z_0}{z_2} \quad (4)$$

$$\Delta\varphi_0 = S_{ax,t} \frac{\tan(\beta_b)}{r_b z_2} \quad (5)$$

In case of a multiple radial infeed strategy, the surface produced in the previous tool pass must also be considered in the calculation (figure 2b), in order to properly describe the material removal and determine the effective material removal.

The local cutting conditions are then calculated for all n points on the cutting tool and all m angular positions along the cutting trajectory and limited to the effective penetration volume. First, the cutting velocity $v_{ci,j}$ and sliding velocities $v_{si,j}$ are calculated. Next, the process angles $\alpha_{i,j}$ and $\gamma_{i,j}$ are calculated from the geometrical relationships between cutting velocity $v_{ci,j}$ and cutting tool geometry. Then, the uncut chip thickness is calculated for each point on the cutting edge as the orthogonal distance from this cutting point to the surface generated by the previous tooth, which is then projected onto the reference plane. The reference plane is defined as the plane through the selected cutting point, perpendicular to the assumed cutting direction [17].

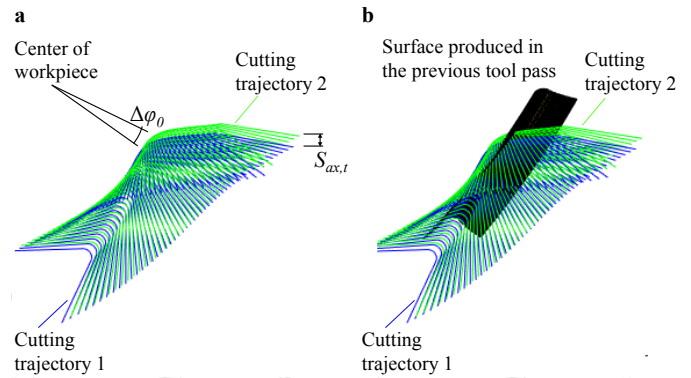


Fig. 2. Calculation of penetration volume: a) comparison of consecutive cutting trajectories; b) surface from previous pass, set as boundary condition.

The specific cutting force is calculated for each local cross section area $A_{c,i,j}$ of the cut element, which is defined as the product between the uncut chip thickness $h_{i,j}$ and the width of cut $b_{i,j}$ (distance between two adjacent points on the cutting edge).

$$F_{c,i,j} = k_{c,i,j} \cdot A_{c,i,j} \quad (6)$$

where

$$A_{c,i,j} = b_j \cdot h_{i,j} \quad (7)$$

The specific cutting force k_c is considered locally and rewritten as a function of the local uncut chip thickness $h_{i,j}$ and the local rake angle coefficient $k_{\gamma,i,j}$. The reference values of specific cutting force for steels can be found in the literature and vary between 1800 and 2100 N/mm² [14, 15]. The specific cutting force $k_{c1,1} = 1800$ N/mm² and the exponent $m_c = 0.26$ are constant in all simulations. It is assumed that the coefficients k_{vc} , k_{chip} and k_{wear} do not vary locally. These are represented by a model fitting coefficient C_m .

$$C_m = k_{vc} \cdot k_{chip} \cdot k_{wear} \quad (8)$$

Finally, the resulting force on each tooth of the cutting tool can be calculated for every cutting tool position i along the cutting trajectory through vectorial addition of the local cutting forces $F_{c,i,j}$ along the cutting edge (see figure 3).

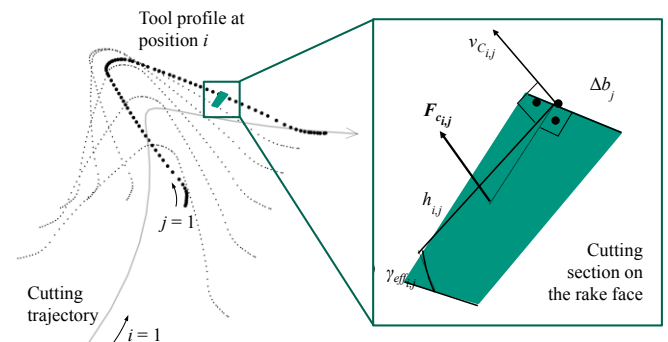


Fig. 3. Graphic representation of the cutting force calculation.

The local cutting force vectors are defined with the same direction as the cutting speed.

$$F_i = \sum_{j=1}^{j=n} k_{c_{i,j}} \cdot A_{c_{i,j}} \quad (9)$$

The equation (9) can be rewritten as:

$$F_i = C_M \cdot k_{c_{1,1}} \cdot \sum_{j=1}^{j=n} b_j \cdot k_{\gamma_{i,j}} \cdot h_{i,j}^{1-m_c} \quad (10)$$

In order to evaluate the most suitable rake angle coefficient, the two methods described in section 1.2 are tested and compared to each other and to the force calculation without considering the influence of the rake angle ($k_\gamma = 1$). For each of the three cases, the correspondent coefficient C_M is adjusted to fit the model.

3. Experimental procedure

The experiments are divided into two sets comprising different parameter windows for skiving of an external gear of non-hardened AISI 5115 Steel (16MnCr5 – 1.7131), with module $m_n = 1.75$ mm, external diameter $d_{2a} = 50.245$ mm and helix angle $\beta_2 = 28.5^\circ$.

The process windows for both sets of experiments are listed in table 1. It can be observed, that two different ranges of axis crossing angle are chosen, in order to variate the kinematics characteristics, leading to different ranges of local rake angle. The minimum local rake angles in the first set of experiments are approximately 50 % than in the second set.

Table 1. Process parameters for the series of experiment.

Set of experiments	Set 1	Set 2
Σ [°]	5 – 15	28.5
β_0 [°]	- 23.5 – - 13.5	0
γ_{tool} [°]	0 – 12	0
α_{tool} [°]	0	7
K [°]	3.3 – 11	0
h_{max} [μm]	40 – 80	40 – 160
v_c [m/min]	50	50
Cutting strategy [passes]	5 – 10	2 – 10
γ_{min} [°]	- 77 – - 36	- 50 – - 20

In the first set of experiments, tests were performed using a single-toothed tool designed for an involute geometry. The cutting tool represents a one tooth segment from a cylindrical skiving tool and one single gap is manufactured in each test. The single-toothed tool and the workpiece geometry are shown in figure 4. Since the cutting tool geometry has no tool clearance angle ($\alpha_{tool} = 0^\circ$), a tilt angle K must be used to create a clearance angle in the process to avoid collision of the tool flank with the workpiece. For every axis crossing angle investigated, a corresponding cutting tool profile and helix angle must be used in order to produce the same desired gear geometry. The cutting tools used are made of powder metallurgical HSS with AlCrN-based coating.

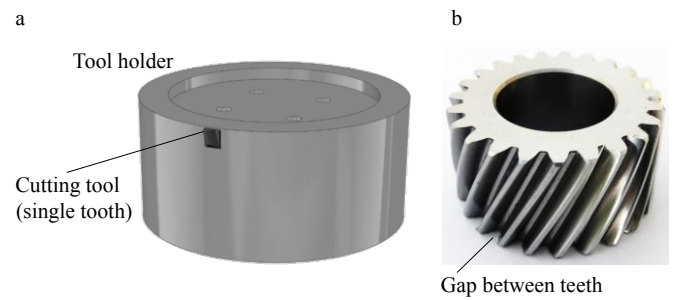


Fig. 4. Experimental setup: a) single-toothed tool and b) gear geometry.

In the second set of experiments, the tests were conducted on the same workpiece geometry using a single-toothed tool with carbide inserts DCMW11T308-RK6 WKK10S. Unlike the cutting tools used in the first set of experiments, the ISO-geometry used does not allow producing an involute profile. Furthermore, this tool has a clearance angle of $\alpha_{tool} = 7^\circ$, representing a tooth of a conical skiving tool. Therefore, no tilt angle K is needed for this set of experiments.

All the tests were conducted in a skiving machine INDEX V300 Sonder with computer numerical control Siemens Sinumerik 840D. The forces were continuously measured on the workpiece spindle in three directions fixed to the rotating workpiece coordinate system using a custom piezo-based Kistler force measuring platform.

A set of raw force measurement data for the second set of experiments is shown in figure 5. Here, the axial feed corresponding to a maximum uncut chip thickness of $h_{max} = 80$ μm is constant for all tool passes. The arithmetic mean of the maximum cutting forces of all single cuts during a tool pass is used as reference to validate the cutting force calculation. Thus, stochastic effects are minimized and each tool pass from a single manufactured tooth gap is a valid data point.

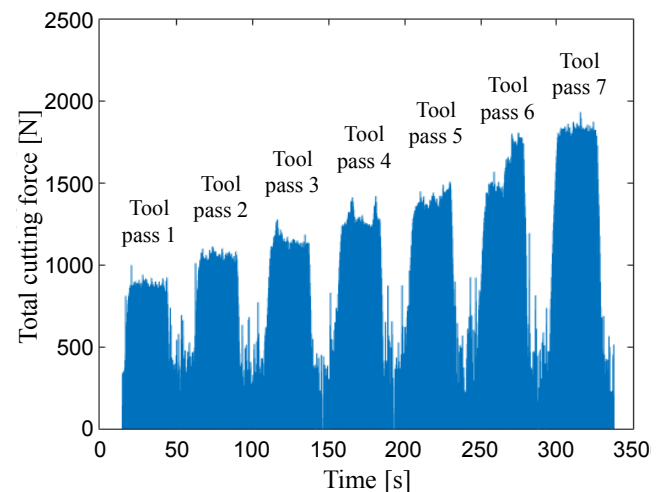


Fig. 5. Exemplary force measurement for 7 tool passes (set of experiments 2).

It can be observed in figure 5, that the cutting forces increase with the cumulated radial infeed, although the maximum uncut chip thickness remains constant. This can be explained by the longer tooth engagement and the following increase of the active contour of the tool profile (analogous to cutting width).

4. Results

In order to compare the different rake angle coefficients k_γ for properly describing the influence of the local rake angle on the cutting forces in gear skiving, the models are fitted to the measured forces in each set of experiments. The two experimental setups are fitted independently, since factors aggregated in the force parameter C_M like tool microgeometry cannot be compared.

A linear regression is used to evaluate the model accuracy for the three cases. The correspondent model fitting coefficient C_M , the maximum error and the coefficient of determination are listed in table 2. The coefficients of determination show good agreement between measured and calculated forces. However, the variation of this parameter is not sufficient to provide a satisfactory comparison between the three models to consider the rake angle. On the other hand, the range of offsets of calculated and measured forces decreases drastically when considering the rake angle through coefficients from literature compared to ignoring it by $k_\gamma = 1$.

Table 2. Model fit for different rake angle coefficients.

Model parameter	Rake Angle coefficient		
	$k_{\gamma,AD}$	$k_{\gamma,GS}$	$k_\gamma = 1$
C_M (set of experiments 1)	0.832	0.736	1.119
C_M (set of experiments 2)	1.654	1.523	1.900
Maximum error	22.6 – 32.0	23.5 – 25.2	24.8 – 47.6
R-squared	0.97	0.96	0.96

For the first set of experiments, the model fitting coefficient C_M is 35 to 50 % higher with $k_\gamma = 1$ than with both rake angle coefficients. For the second set of experiments, the relation between the model fitting coefficients C_M for $k_\gamma = 1$ and the calculated rake angle coefficients is smaller. The model fitting coefficient C_M is 15 to 25 % higher with $k_\gamma = 1$ than with the two rake angle coefficients.

The similar coefficients of determination and the higher error for the force calculations with $k_\gamma = 1$ may suggest that the effect of the rake angle is indirectly compensated by the model fitting coefficient. However, considering the rake angle by a given coefficient increases the accuracy of the force model.

In order to compare the different methods to calculate the rake angle coefficient, the maximum error is evaluated. For the first set of experiments, the best results are achieved with $k_{\gamma,GS}$. According to this method, the influence of the rake angle on the cutting forces results in 1.5 % force increase per degree rake angle decrease. For the second set of experiments, the best results are achieved using $k_{\gamma,AD}$. Here, the influence of the rake angle on the cutting forces is moderate, where each degree rake angle change results by a 1 % force increase. The results for both $k_{\gamma,GS}$ and $k_{\gamma,AD}$ are shown in figure 6.

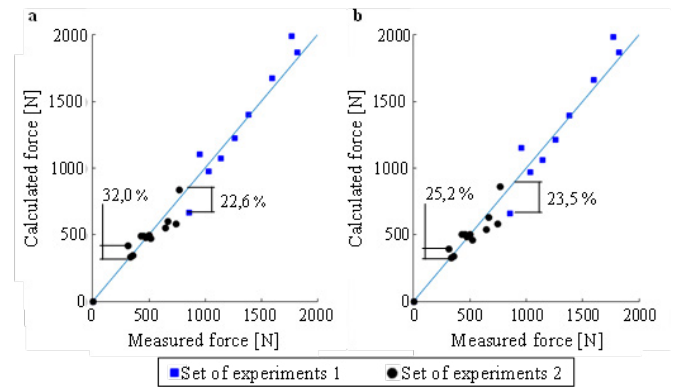


Fig. 6. Comparison of calculated and measured forces for: a) $k_{\gamma,AD}$, b) $k_{\gamma,GS}$.

As can be observed in figure 6, the rake angle coefficient $k_{\gamma,GS}$ (right) is more suitable for the cutting forces calculation concerning the first set of experiments, where the axis crossing angles investigated are smaller and the local rake angles inherent to the unfavorable kinematics reach lower values. On the other hand, the rake angle coefficient $k_{\gamma,AD}$ (left) shows a slightly better model accuracy for the parameters investigated in the second set of experiments.

5. Conclusion

A numerical model was developed to calculate the cutting forces by gear skiving. This model considers the variation of the local cutting conditions inherent to the skiving kinematics and especially includes the influence of the local rake angle based on an extended Kienzle equation of cutting forces.

In order to validate the model, two sets of experiments with different parameter ranges were tried. Two different approaches for the calculation of the rake angle coefficient [13, 14, 15, 16] were implemented in the numerical model and tested. The calculation results are also compared to results without a rake angle coefficient.

A linear regression is used to evaluate the model accuracy. In all three variants of the force calculation, the high coefficient of determination of the linear regression indicates a good agreement between measured and calculated data. The differences of coefficient of determination is not sufficient to provide a satisfactory comparison between the different modelling approaches. On the other hand, the comparison between measured and calculated forces show a reduction of the maximum error from 47 % to 32 % by considering the rake angle coefficient.

Both tested methods to consider the influence of the rake angle lead to more accurate results compared to the results achieved with the standard force model. Thus, the results show that considering the effect of the local rake angle in the cutting force calculation reduces the maximum error and enhances the model accuracy. This is especially relevant for machining processes with a high variation of the rake angle during tool engagement like gear skiving.

The comparison of the two calculation methods of the rake angle coefficients shows slight differences. The first one, described by Apprich et al. [14] and Dietrich [15], considers an increase of 1 % of the cutting force for each degree change of

the rake angle and shows the best results for the second set of experiments. The second one, described by Saglam et al. [13] and Günay [16], considers an increase of 1.5 %. This is better suited to calculate forces for the first set of experiments. This can be explained by the overall less negative values of rake angle in the second set of experiments, indicating that a non-linear rake angle coefficient may be more suitable for calculating the cutting forces by gear skiving. In further investigations, the influence of rake angles $-80^\circ < \gamma < -20^\circ$ on the cutting forces should be investigated in greater detail.

Acknowledgements

The presented results were achieved in research project FVA 661 II: „Gear Skiving with Reduced Axis Crossing Angles“ sponsored and supported by Forschungsvereinigung Antriebstechnik e.V. (FVA) and Arbeitsgemeinschaft industrieller Forschungsvereinigungen „Otto von Guericke“ e.V. (AiF).

References

- [1] Pittler von W (1910) Verfahren zum Schneiden von Zahnrädern mittels eines zahnradartigen, an den Stirnflächen der Zähne mit Schneidkanten versehenen Schneidwerkzeugs. Patent specification.
- [2] Jansen W (1980) Leistungssteigerung und Verbesserung der Fertigungsgenauigkeit beim Wälzschälen von Innenverzahnungen. Dissertation RWTH Aachen.
- [3] Hühsam A (2002) Modellbildung und experimentelle Untersuchung des Wälzschälprozesses. Dissertation, Universität Karlsruhe.
- [4] Kühlewein, C (2013): Untersuchung und Optimierung des Wälzschälverfahrens mit Hilfe von 3D-FEM-Simulation. 3D-FEM Kinematik- und Spanbildungssimulation. In: Forschungsberichte aus dem wbk, Institut für Produktionstechnik, Universität Karlsruhe (TH).
- [5] Klocke F, Brecher C, Löpenhaus C, Ganser P, Staudt J, Krömer M (2016) Technological and simulative analysis of power skiving. *Procedia CIRP* 50: p. 773-778.
- [6] Tsai C.Y. (2016) Mathematical model for design and analysis of power skiving tool for involute gear cutting. *Mechanism and Machine Theory* 101, p: 185-208.
- [7] Bauer R, Putz M, Hochmuth C (2016) Modellbasierte Optimierung der Prozessführung beim Wälzschälen. 6th GETPRO.
- [8] Guo Z, Mao S.M., Huyan L, Duan D.S. (2018) Research and improvement of the cutting performance of skiving tool. *Mechanism and Machine Theory* 120: p. 302-313.
- [9] Spath D, Hühsam A (2002) Skiving for high-performance machining of periodic structures. Vol. 51, Issue 1, p. 91-94.
- [10] Li J, Wang P, Jin Y, Hu Q, Chen X.C. (2016) Cutting force calculation for gear slicing with energy method. *The International Journal of Advanced Manufacturing Technology*, Vol. 83 (5-8): p. 887-896.
- [11] Markopoulos A.P., Karkalos N.E., Vaxevanidis N.M. Manolakos D.E. (2016) Friction in Orthogonal Cutting Finite Elements Models with Large Negative Rake Angle. *Tribology in Industry*, Vol. 38, No. 2, p. 214-220.
- [12] Fang N. (2005) Tool-chip friction in machining with a large negative rake angle tool. *Wear* 258: p. 890-897.
- [13] Saglam H., Unascar F., Yaldiz S. (2006) Investigation of the effect of rake angle and approaching angle on main cutting force and tool tip temperature. *International Journal of Machine tools & Manufacture* 46: p. 132-141.
- [14] Apprich T, Heine B, Liesch J, Brenner J, Hochstatter A, Pflug A, Dambacher M, Holzberger S, Schmid D, Dreher F, Holzwarth F, Tawakoli T, Fischer G, Kaiser H, Vogel R, Greiner G (2016) Tabellenbuch für Zerspantechnik. 2nd Edition, Verlag Europa-Lehrmittel, Haan-Gruiten.
- [15] Dietrich J. (2016) Grundlagen der Zerspaltung am Beispiel Drehen. In: *Praxis der Zerspantechnik*. Springer Vieweg, Wiesbaden.
- [16] Günay M., Seker U. (2005) Kesici Takım Talaş Açısının İlerleme Kuvveti Üzerindeki Etkisinin Araştırılması. *Journal of Polytechnic* Vol. 4, No. 4, p. 323-328.
- [17] ISO 3002-1 (1982) Basic quantities in cutting and grinding – Part 1: Geometry of the active part of cutting tools – General terms, reference systems, tool and working angles, chip breakers.